TITLE

Biomineralisation plasticity and environmental heterogeneity predict geographic resilience patterns of foundation species to future change

Running title

Shell plasticity predicts resilience

List of authors

Luca Telesca,[1,2] Lloyd S. Peck,[2] Trystan Sanders,[3] Jakob Thyrring,[2,4] Mikael K. Sejr,[5,6] Elizabeth M. Harper[1]

Institutional affiliations

[1] Department of Earth Sciences, University of Cambridge, CB2 3EQ Cambridge, UK.

[2] British Antarctic Survey, CB3 0ET Cambridge, UK.

[3] GEOMAR Helmholtz Centre for Ocean Research, 24105 Kiel, Germany.

[4] Department of Zoology, University of British Columbia, V6T 1Z4, Vancouver, BC, Canada

[5]Department of Bioscience, Arctic Research Centre, Aarhus University, 8000 Aarhus C, Denmark.

[6] Department of Bioscience, Marine Ecology, Aarhus University, 8600 Silkeborg, Denmark.

Contact Information

Luca Telesca, email: lt401@cam.ac.uk, phone: +44 (0) 1223 33408

Elizabeth M. Harper, email: emh21@cam.ac.uk, phone: +44 (0) 1223 333428

ABSTRACT

Although geographic patterns of species' sensitivity to environmental changes are defined by interacting multiple stressors, little is known about compensatory processes shaping regional differences in organismal vulnerability. Here, we examine large-scale spatial variations in biomineralisation under heterogeneous environmental gradients of temperature, salinity, and food availability across a 30° latitudinal range (3,334 km), to test whether plasticity in calcareous shell production and composition, from juveniles to large adults, mediates geographic patterns of resilience to climate change in critical foundation species, the mussels *Mytilus edulis* and *M. trossulus*. We find shell calcification decreased towards high latitude, with mussels producing thinner shells with a higher organic content in polar than temperate regions. Salinity was the best predictor of within-region differences in mussel shell deposition, mineral and organic composition. In polar, subpolar, and Baltic low-salinity environments, mussels produced thin shells with a thicker external organic layer (periostracum), and an increased proportion of calcite (prismatic layer, as opposed to aragonite) and organic matrix, providing potentially higher resistance against dissolution in more corrosive waters. Conversely, in temperate, higher-salinity regimes, thicker, more calcified shells with a higher aragonite (nacreous layer) proportion were deposited, which suggests enhanced protection under increased predation pressure. Interacting effects of salinity and food availability on mussel shell composition predict the deposition of a thicker periostracum and organic-enriched prismatic layer under forecasted future environmental conditions, suggesting a capacity for increased protection of high-latitude populations from ocean acidification. These findings support biomineralisation plasticity as a potentially advantageous compensatory mechanisms conferring *Mytilus* species a protective capacity for quantitative and qualitative trade-offs in shell deposition as a response to regional alterations of

abiotic and biotic conditions in future environments. Our work illustrates that compensatory mechanisms, driving plastic responses to the spatial structure of multiple stressors, can define geographic patterns of unanticipated species resilience to global environmental change.

Keywords

Climate change, *Mytilus*, calcification, biomineralisation, resistance, ocean acidification, compensatory mechanisms, multiple stressors

INTRODUCTION

Unprecedented global environmental changes are driving scientists towards increased efforts to investigate the mechanisms underlying geographic variation in biotic responses to future environmental conditions (Nagelkerken & Connell, 2015; Urban et al., 2016). However, our ability to predict changes to species and ecosystems in response to climate change remains limited (Kroeker, Kordas, & Harley, 2017). Current projections are severely constrained by heterogeneous patterns of ocean warming and acidification (Gattuso et al., 2015), multiple stressors (Breitburg et al., 2015), and compensatory processes (Cross, Harper, & Peck, 2019; Ghedini, Russell, & Connell, 2015; Leung, Russell, & Connell, 2017), as well as predictive models which often exclude important biological mechanisms (Urban et al., 2016). Therefore, a better mechanistic understanding of environmental sources and processes mediating species' responses to disturbances is critical for building the theoretical baseline necessary to forecast the combined effects of multiple emerging stressors (Kroeker et al., 2017; Urban et al., 2016).

Advances in macroecology suggest that permanent environmental mosaics, defined by spatial overlaps of non-monotonic environmental gradients (Kroeker et al., 2016), as well as regional adaption or acclimatisation (Calosi et al., 2017; Peck, 2018; Vargas et al., 2017), dictate geographic variations in species performance and sensitivity to disturbances in marine ecosystems. Key to these works is that responses vary among populations and taxa (Calosi et al., 2017; Kroeker et al., 2013; Telesca et al., 2018), which often play disproportionately strong roles in structuring benthic communities (Ashton, Morley, Barnes, Clark, & Peck, 2017). Thus, species-specific biological processes driving organismal variability likely shape differential regional responses of foundation species to co-occurring multiple drivers. This can establish

spatial patterns of unexpected susceptibility of marine communities to future environmental conditions.

Species producing calcium carbonate ($CaCO_3$) shells and skeletons are possibly experiencing the strongest impacts of rapid environmental changes (Kroeker et al., 2013). Knowledge of their sensitivity is derived largely from short- to long-term studies on model organisms (Kroeker et al., 2013; Nagelkerken & Connell, 2015), while complex variations under multiple stressors in natural environments have rarely been investigated (Ashton et al., 2017; Kroeker et al., 2016; Peck et al., 2015; Watson, Morley, & Peck, 2017). Therefore, inferences made from experimental studies may not necessarily translate to complex marine ecosystems (Connell et al., 2017; Vargas et al., 2017). Indeed, species-specific responses to habitat alterations (Kroeker et al., 2013), on top of mixed outcomes of environmental interactions (Crain, Kroeker, & Halpern, 2008), make future ecosystem predictions extremely challenging (Kroeker et al., 2017). This leaves open the question: do differences in biological processes, shaping regional variations of calcifiers' responses to interacting environmental stressors, define geographic patterns of unanticipated species sensitivity or resilience to global environmental change?

A body of research has focused on responses of marine calcifiers to altered water chemistry (Kroeker et al., 2013; Nagelkerken & Connell, 2015), but studies have rarely considered changes in biogeochemical cycles strongly mediating biological responses to disturbance (Gattuso et al., 2015). Among those, a marked intensification of the global water cycle in response to warming (+4% for +0.5 °C) has been documented over recent decades through changes in ocean salinity (Durack, Wijffels, & Matear, 2012). Salinity is a major ecological factor dictating distribution and survival of aquatic organisms, ecosystem functioning (Solan & Whiteley, 2016), as well as conditions for biomineralisation (Thomsen, Haynert, Wegner, & Melzner, 2015). Indeed, salinity

correlates positively with the availability of calcification substrates [bicarbonate (HCO_3^-) and calcium (Ca^{2+}) ion concentrations] and, therefore, seawater $CaCO_3$ saturation state (Ω_{CaCO_3}) (Thomsen, Ramesh, Sanders, Bleich, & Melzner, 2018). Saturation states of the two main $CaCO_3$ polymorphs [calcite (Ω_{calc}) and aragonite (Ω_{arag})] control calcification kinetics, driving net deposition or dissolution of $CaCO_3$ structures (Ries, Ghazaleh, Connolly, Westfield, & Castillo, 2016; Sanders, Schmittmann, Nascimento-Schulze, & Melzner, 2018; Thomsen et al., 2018). Multidecadal studies have revealed a global salinity pattern following the "rich-get-richer" mechanism, where salty ocean regions (compared to the global mean) are getting saltier (mid-latitudes), whereas low salinity regions are getting fresher (tropical convergence zones and polar regions) (Durack et al., 2012). In a future 2 - 3 °C warmer world, a substantial 16 - 24% intensification of the global water cycle is predicted to occur, making salinity gradients much sharper (Durack et al., 2012). This may affect deposition rates of biogenic $CaCO_3$ through altered calcification costs. However, the emergent ecological effects of changing salinity on calcifying species are largely unknown.

Atlantic blue mussels, *Mytilus edulis* and *M. trossulus*, are important bed-forming foundation species throughout the eulittoral ecosystems of the northern hemisphere, and represent valuable resources for aquaculture (192,000 t produced in 2016 worth 325 million USD) (FAO, 2017). Growing awareness of the consequences of climate change on biodiversity and the industry that *Mytilus* species support has stimulated a number of studies to estimate their response potential to changing ocean conditions (Telesca et al., 2018; Thomsen et al., 2017; Thyrring, Blicher, Sørensen, Wegeberg, & Sejr, 2017).

Calcareous shells perform a range of vital functions including structural support and protection against predators. Because shell integrity determines survival, shell traits are subject to strong

selection pressure with functional success or failure a fundamental evolutionary driver. Blue mussel shell consists of three layers (Fig. 1a,b): (1) the outer organic periostracum, and the calcified (2) anvil-type fibrous prismatic and (3) nacreous layers. The periostracum is made of sclerotised (quinone-tanned) proteins. This layer provides a protected environment for the deposition of calcareous components, and protects shells from corrosive, acidic waters as well as predatory and endolithic borers (Harper, 1997). The fibrous prismatic and nacreous layers are composed of $CaCO_3$ crystals of different mineral forms, calcite and aragonite respectively, and inter-crystalline biomineral organic matrix (Checa, Pina, Osuna-Mascaró, Rodríguez-Navarro, & Harper, 2014). These calcareous layers are characterised by different microstructures (Fig. S1) and more (i.e. aragonite) or less (i.e. calcite and organics) soluble components (Harper, 2000; Mucci, 1983), the combination of which determines specific chemical and mechanical shell protection characteristics (Barthelat, Rim, & Espinosa, 2009; Currey & Taylor, 1974; Fitzer et al., 2015). Differences in energetic costs of making shell components (Palmer, 1992; Watson et al., 2017), combined with future alterations in environmental gradients (Gattuso et al., 2015) and water carbonate chemistry (Thomsen, et al., 2015; Thomsen et al., 2018), will likely influence variations in shell production and composition, shaping regional patterns of shell resilience to abiotic and biotic alterations.

Mytilus spp. growth, biomineralisation and fitness are linked to multiple drivers, including water temperature, salinity and food supply [chlorophyll-*a* (Chl-*a*) concentration] (Sanders et al., 2018; Thomsen, Casties, Pansch, Körtzinger, & Melzner, 2013). As is the case for all, but in the context of this study, in the North Atlantic and Arctic Oceans these key environmental factors vary heterogeneously with latitude (Fig. 1c,d), encompassing a range of conditions predicted under different future climate change scenarios (Kirtman et al., 2013). Here, we hypothesise that

plasticity in shell biomineralisation, driving spatial variations in shell production, mineral and organic composition, i) shape regional responses of *Mytilus* species to interacting environmental drivers, and ii) define geographic patterns of blue mussel vulnerability in the face of global environmental changes.

Despite projected alterations of salinity (Durack et al., 2012; Gattuso et al., 2015) and, therefore, water carbonate chemistry (Ω_{CaCO_3}) and calcification costs (Sanders et al., 2018; Thomsen et al., 2018), salinity gradients have been overlooked in large-scale predictive models for marine calcifiers. This knowledge is essential to forecast whether environmental changes affect shell variability and functional capability, especially in ecologically important foundation species such as *M. edulis* and *M. trossulus*. These factors are crucial for understanding species susceptibility to other rapidly emergent stressors, such as warming, acidification, and altered species interactions (Kroeker et al., 2017).

In this study, we examine the relationships between variations in *Mytilus* spp. shell biomineralisation, from juveniles to large adults, and interactive environmental gradients of temperature, salinity and Chl-*a* concentration in 17 populations spanning a latitudinal range of 30° (3,334 km) across the Atlantic-European and Arctic coastline (Fig. 1c,d). In particular, we tested for a latitudinal effect on blue mussel shell calcification that we hypothesise will show a general decrease from temperate to polar regions. We also identified environmental sources of within-region variations in shell production and composition, to test whether salinity affects shell biomineralisation during growth, suggesting changes of shell structure, mechanical and chemical properties. Finally, we modelled spatial trends in shell deposition with environmental gradients, to test whether plasticity in shell biomineralisation shapes regional responses of *Mytilus* species to interacting stressors, defining geographic patterns of sensitivity to future changes.

MATERIALS AND METHODS

Mytilus collection

We sampled individuals from 17 *Mytilus* (*M. edulis* and *M. trossulus*) populations along the North Atlantic, Arctic, and Baltic Sea coastlines from four distinctive climatic regions (warm-temperate, cold-temperate, subpolar and polar) covering a latitudinal range of 30° (a distance of 3,334 km), from Western European (Brest, North-West France, 48°N) to Northern Greenlandic (Qaanaaq, North-West Greenland 78°N) coastlines (Fig. 1c). During December 2014 - September 2015, mussels of various size classes for each site (shell length 26 - 81 mm) were sampled from the eulittoral zone on rocky shores for a total of 424 individuals (Table S1). At each site, specimens were collected from the lower limit of the intertidal zone (0 - 0.5 m above the zero tidal level) on rocky substratum to allow for comparisons (in terms of local conditions) between Atlantic and Baltic mussels, the latter experiencing short and irregular periods of air exposure during the year. For each specimen, shell length was measured with digital calipers (0.01 mm precision) and used as a within-population (collection site) proxy for age (Seed & Richardson, 1990).

We analysed *Mytilus* populations for which the genetic structure was known, with particular focus on species identity and hybrid status (*M. edulis* × *M. trossulus*). Genetic studies have revealed various episodes of extensive introgression of *M. edulis* alleles in *M. trossulus* populations and pronounced hybridisation patterns, especially in the Baltic Sea (Riginos & Cunningham, 2005; Stuckas, Stoof, Quesada, & Tiedemann, 2009), resulting in the absence of "pure" *M. trossulus* populations at the North Atlantic and Baltic Sea scales. *Mytilus* shells used were either from individuals already evaluated in genetic investigations or mussels obtained

from sites routinely used in regional monitoring programs that provided information on genetic status (Table S1). Areas where the Mediterranean mussel, *Mytilus galloprovincialis*, was known to be present were avoided. We did, however, sample a few sites (3) with very low levels of *M. edulis* × *M. galloprovincialis* hybridisation. Here, mussels from the *M. edulis* species-complex were analysed together because: i) they share the same shell microstructure (Fig. S1), ii) they inhabit a wide range of similar habitats in the eulittoral zone, iii) their pervasive hybridisation patterns (with differential introgression) excluding pure *M. trossulus* populations at the spatial scale analysed, and **iv**) the documented smaller contribution of genetic status than environmental heterogeneity on the variability of *Mytilus* shell traits across large geographic scales (Krapivka et al., 2007; Telesca et al., 2018).

Mussel shell preparation

We set left shell valves in polyester resin (Kleer-Set FF, MetPrep, Coventry, U.K.) blocks. Embedded specimens were sliced longitudinally along their axis of maximum growth (Fig. 1a) using a diamond saw and then progressively polished with silicon carbide paper (grit size: P800 - P2500) and diamond paste (grading: 9 - 1 µm). Photographs of polished sections (Fig. 1b) were acquired with a stereo-microscope (Leica M165 C equipped with a Leica DFC295 HD camera, Leica, Wetzlar, Germany) and shell thickness was measured using the Fiji software (v1.51w). Since larger individuals had undergone evident environmental abrasion or dissolution which removed the periostracum and prismatic layer closer to the umbo, we estimated the thickness of the whole-shell, prismatic and nacreous layers at the midpoint along the shell cross-section. Periostracum thickness was measured at the posterior edge where it attaches to the external side

of the prismatic layer, to estimate the fully formed organic layer that was unaffected by decay or abrasion (Harper, 1997).

Organic content analyses

We performed thermogravimetric analyses (TGA) to estimate the weight proportion (wt%) of organic matrix within the prismatic layer. A random subsample of 20 *Mytilus edulis* specimens were selected from four populations (sites 1, 11, 15, 16) to explore differences in shell organic content under temperate and polar regimes. We removed the periostracum by sanding, and tiles of prismatic layer (8 × 5 mm, $n = 20 \times 4$ sites) were cut along the posteroventral shell margin. Tiles were cleaned, air-dried and then finely ground. We tested ten milligrams of this powdered shell with a thermogravimetric analyser (TGA Q500, TA Instruments, New Castle, DE, U.S.A.). Samples were subjected to constant heating from ~25 °C to 700 °C at a linear rate of 10 °C min^{-1} under a dynamic nitrogen atmosphere and weight changes were recorded (Supporting Document S1). We estimated the wt% of organic matter within the shell microstructure as the proportion of weight loss during the thermal treatment between 150 °C and 550 °C (Fig. S2). The TGA method was used in preference to the traditional muffle furnace approach to explore changes in organic matrix within a specific shell layer (intra- and inter-crystalline organics). Although traditional approaches are still used to measure variation of organic content at the whole-shell level (i.e. estimates of total organics including organic matrix, shell ligament and organics-rich layers, such as the periostracum and myostracum) (Sanders et al., 2018), TGA represents a more accurate and widely used method to provide an unbiased estimate (i.e. no influence of residual intracrystalline water) of the wt% of organic matrix at a single microstructure level in molluscs

(Checa, Macías-Sánchez, Harper, & Cartwright, 2016; Zaremba, Morse, Mann, Hansma, & Stucky, 1998). In a cross calibration experiment where samples of blue mussel shells were analysed both in a muffle furnace and by TGA (n = 5 × 4 sites), results obtained were not significantly different (Fig. S3).

Environmental characterisation

We selected three key environmental drivers based on their known influence on mussel growth and calcification, their level of collinearity across the geographic scale investigated, and the forecasted major ocean alterations under climate change (Kirtman et al., 2013; Sanders et al., 2018; Thomsen, et al., 2013). For each site measurements of sea surface temperature, salinity, and Chl-*a* concentration, the latter being used as a proxy for food supply (Thomsen, et al., 2013), were generated using the Copernicus Marine Environment Monitoring Service (CMEMS) (http://marine.copernicus.eu/). These climate datasets are composed of high-resolution physical and biogeochemical assimilated (iterative integration of new observational information and model forecasts over time) daily data (Supporting Document S2). To provide a first order mean approximation of the average water conditions prevailing during the periods of mussel growth and shell deposition (Carter & Seed, 1998; Thomsen, et al., 2010) across the life-span of both young and adult sampled specimens from different age classes (between two and six years old), we expressed parameters as mean May - October values averaged over the 6-year period 2009 - 2014 (daily observation, n = 2,191 per parameter) and used these as input variables (Fig. 1d; Table S2).

Direct environmental monitoring for each site was not feasible due to the number and geographic range (> 3,300 km latitudinal span) of the mussel populations analysed, the absence of direct records for many of the sites used, and the temporal resolution (daily data over six years) required to provide an average estimate for the growth conditions of young and adult specimens. For this large-scale study, assimilated data presented potential advantages compared to traditional measurements due to their spatial and temporal extent, repetition over time, advanced calibration and validation (i.e. high correlation with discrete field measurements) (IOCCG, 2014; Telesca et al., 2018; Thomas et al., 2011).

Statistical analysis

Generalised linear (mixed) models, GL(M)Ms, were used to explain shell thickness and composition, from juveniles to large adults, with respect to latitude and environmental drivers, and to compare between the individual shell layers. GLMMs were applied i) to account for the hierarchical structure of the dataset consisting of multiple specimens (n = 24 - 26 replicates) from each collection site, ii) to control for variations ("noise") among sampling units (collections sites) due to local habitats, and iii) to generalise our results to Atlantic *Mytilus* populations beyond the study sample (Bolker, 2015; Zuur, Ieno, Walker, Saveliev, & Smith, 2009).

We carried out data exploration following the protocol of Zuur et al. (2010). Initial inspection revealed no outliers. Pairwise scatterplots and variance inflation factors (VIFs) were calculated to check for collinearity between input variables. VIF values < 2 indicated an acceptable degree of correlation among covariates to be included within the same model. We applied residual regression to uncouple the unique from the shared contribution of temperature and Chl-*a*

concentration to the response (Graham, 2003). This allowed us to account for the existing causal link between these two parameters and to avoid inferential problems from modelling non-independent covariates without losing explanatory power (Graham, 2003). To directly compare model estimates (effect size metrics) from predictors on different measurement scales, to estimate biologically meaningful intercepts, and to interpret main effects when interactions are present, we standardised all the input variables (environmental parameters and shell length) (Grueber, Nakagawa, Laws, & Jamieson, 2011; Schielzeth, 2010). For standardisation, we subtracted the sample mean from the variable values and divided them by the sample standard deviation $[z_i = (x_i - \bar{x})/\sigma_x]$ (Schielzeth, 2010).

We used separate GLMMs to explore patterns of whole-shell and periostracum thickness with latitude, environmental conditions, and shell length (size) (n = 424). A different approach was used to investigate relationships between calcareous layers and latitudinal gradients. Prismatic and nacreous layer thickness were analysed within the same GLMM (n = 424 × 2 layers) to i) estimate their variation and covariation across latitudes, ii) predict simultaneously common and divergent environmental effects on both layers, and iii) reduce the probability of type I error. To model the relationship between layer thickness and latitude we used a GLMM with a normal distribution with latitude (continuous), shell layer (categorical, two levels: prismatic and nacreous) and their interaction as fixed covariates. To model shell thickness as a function of the environmental predictors we used a GLMM with a normal distribution (Equation 1). In the initial model, fixed continuous covariates were standardised temperature, salinity and Chl-*a* in addition to shell layer (categorical, two levels) and their two-way interactions. Shell length (continuous) was included in both models to control for possible effects of within-population size variation on layer thickness. To incorporate the dependency among observations for a specific layer from the

same collection site, we used site as a random intercept. Preliminary inspection of models' residuals showed heteroscedasticity in most models. The use of different continuous probability distributions (i.e. gamma and inverse Gaussian) and link functions did not stabilise the variance, therefore a ln-transformation of the response was required. Response variables did not require further transformations.

The proportion (wt%) of organic matrix in the prismatic layer (n = 80) was modelled with GLMs as a function of collection site (categorical, four levels) and prismatic thickness (continuous) to test for differences between polar and temperate regions and association with shell thickness. The response variable was coded as a value from 0 to 1; therefore, we used a GLM with a beta distribution and a logistic link function. Pair-wise contrasts with a standard Bonferroni correction (alpha of 0.0125) were then used to test for differences in wt% among sites within and between climatic regions.

Models were optimised by first selecting the random structure and then the optimal fixed component. The principal tools for model comparison were the corrected Akaike Information Criterion (AICc) and bootstrapped likelihood ratio tests. Random terms were selected on prior knowledge of the dependency structure of the dataset. Visual inspection of residual patterns indicated violation of homogeneity in most cases. This required the use of variance structures (generalised least squares) allowing the residual spread to vary with respect to shell layer. The fixed component was optimised by rejecting only non-significant interaction terms that minimised the AICc value. For all model comparisons, variation of AICc between the optimal (lowest AICc value) and competing models were greater than 8, and fixed-effect estimates were nearly identical, indicating that competing models were very unlikely to be superior (Burnham & Anderson, 2002). The proportion of variance explained by the models was quantified with

conditional or pseudo determination coefficients (cR^2 or $pseudoR^2$) (Nakagawa, Johnson, & Schielzeth, 2017). We used variograms to assess the absence of spatial autocorrelation. Final models were validated by inspection of standardised residual patterns to verify GLMM assumptions of normality, homogeneity and independence. We used optimal models fitted on standardised input variables (same measurement scale) to estimate the mean effect sizes of environmental drivers on the response (Schielzeth, 2010). Ninety-five per cent confidence intervals (95% CIs) for the regression parameters were generated using bias-corrected parametric bootstrap methods (10,000 iterations). 95% CIs were used for statistical inference due to estimation of approximated significance values (*p*-value) in mixed-modelling. If the confidence intervals did not overlap zero, then the effect was considered significant. Conditional modes and variances of the random effect were calculated for each GLMM to inspect differences in collection site-level effect on the variation of individual layer thickness after accounting for the effect of environmental covariates and shell size (fixed component). All data exploration and statistical modelling were performed in R (v3.4.1) (for packages see Table S3).

A principal component analysis (PCA), with a singular value decomposition method, was performed on shell traits (i.e. thickness of prismatic layer, nacreous layer, and periostracum) to observe variations in shell composition among individuals from different climatic regions. The PCA was used to create new independent variables, the principal components (PCs), resulting from the linear combinations of shell traits (Table S4), and to observe how these changed together among populations.

RESULTS

Latitudinal patterns of shell deposition

GLMMs indicated a general decrease of *Mytilus* whole-shell thickness with increasing latitude (95% CI = –0.36 to –0.01, $cR^2 = 0.81$) (Fig. 2, S4). We detected a significant negative relationship between the prismatic and nacreous layers thickness and latitude (95% CI = –0.258 to –0.068, $cR^2 = 0.71$; Fig. 2, S4), while no variation in periostracum thickness (95% CI = –0.14 to 0.07, $cR^2 = 0.81$; Fig. 2) was detected. No significant change in the relative thickness of prismatic and nacreous layers was observed across the sampled latitudinal range (latitude × layer interaction, 95% CI = –0.24 to 0.15; Table S5). Shell length was positively correlated with thickness in all layers indicating thickening during growth (Fig. 2; Table S5).

Prismatic layers were characterised by a significantly higher wt% of organic content (lower proportion of $CaCO_3$) in mussel shells from polar than temperate regions, indicating decreased shell calcification at high latitudes (Fig. 3a, S3). Polar shells [sites 15, 16; mean (SD) = 1.8 wt% (0.31)] were characterised by an average of 29% more organic content compared to temperate mussels [sites 1, 11; mean (SD) = 1.4 wt% (0.16)]. The wt% of organics was negatively correlated with prismatic thickness (Fig. 3b), indicating a lower proportion of $CaCO_3$ and thinner, less calcified, shells at polar latitudes.

Environmental influence on shell production and composition

We identified significant trends in shell thickness with environmental gradients depending on the shell measurement considered (Fig. 2, S5; Table 1). Whole-shell thickness was positively related

to temperature, salinity and shell length, but there was no influence of Chl-*a* ($cR^2 = 0.93$; Fig. 2). Salinity had an effect on shell thickness that was 3.4 and 2.1 times larger than temperature and length, respectively (Fig. 2; Table 1).

Prismatic and nacreous layer thicknesses were analysed within the same GLMM. After model selection, fixed continuous covariates of the optimal model, Equation (1), were standardised *temperature*, *salinity*, *Chl-a*, shell *length* in addition to shell *layer* (categorical, two levels: prismatic and nacreous) and the *salinity* × *layer*, *length* × *layer* interactions. The random component was collection *site* used as a random intercept. The model was of the form:

$$\ln\left(Thickness_{ijk}\right) \sim N\left(\mu_{ijk}; \sigma_j^2\right)$$

$$\mu_{ijk} = Temperature_{ik} + Salinity_{ik} + Chl\text{-}a_{ik} + Length_{ik} + Layer_j + Salinity_{ik} \times Layer_j + Length_{ik} \times Layer_j + Site_{ij}$$

$$Site_{ij} \sim N(0; \sigma_{Site}^2)$$

(Equation 1)

where $Thickness_{ijk}$ is the *k*th thickness observation from layer *j* (*j* = prismatic, nacreous) and site *i* (*i* = 1,…, 17). $Site_{ij}$ is the random intercept for layer *j*, which is assumed to be normally distributed with expectation 0 and variance σ_{Site}^2.

Sea surface temperature, salinity and shell length all successfully predicted ($cR^2 = 0.93$) variations in the thickness of prismatic and nacreous layers, while no influence of Chl-*a* on either layer was detected (Table 1). The mean effect size of salinity on the response was twice as large as the effect of shell length, while it was 2.9 and 4.7 times larger than the effect of temperature on the prismatic and nacreous layers, respectively (Equation 2; Fig. 2). This indicates salinity

had a stronger contribution to predicting shell structure than the effects of temperature, Chl-*a*, and shell length combined (Fig. 4).

$$\mu_{ijk} = \begin{cases} 5.907 + 0.138 \times Temperature + 0.396 \times Salinity + 0.028 \times Chl\text{-}a + 0.197 \times Length & \text{Prismatic} \\ 5.853 + 0.138 \times Temperature + 0.654 \times Salinity + 0.028 \times Chl\text{-}a + 0.308 \times Length & \text{Nacreous} \end{cases}$$

(Equation 2)

Interactions between shell layer and both salinity and shell length (Equation 2) indicate deposition of proportionally thicker prismatic layers (higher proportion of calcite) under low salinities and proportionally thicker nacreous layers (higher proportion of aragonite) under higher salinities across the entire range of shell lengths (Fig. 4). No change in the relative thickness of prismatic and nacreous layers with water temperature was detected (Table S6).

Periostracum variability

Models of periostracum thickness revealed significant exponential relationships with Chl-*a* and shell length ($cR^2 = 0.81$) (Table 1). Length had a mean effect that was three times larger than Chl-*a* (Fig. 2), showing a rapid thickening of the periostracum during shell growth. The interactions between shell length and both salinity and temperature indicate that the effects of these variables on the periostracum were interdependent. At low salinities, the higher values of shell length had a greater positive effect on periostracum thickness, while the reverse was true for higher temperatures which had a marginal effect only on thickening rates (Fig. 5a, S6). This suggests that periostracum thickening during shell growth was faster in fresher waters than in relatively saltier conditions.

Among-site shell variation

GLMMs showed no difference in collection site-level effects (conditional modes) on each thickness measurement (Fig. 5b). Conditional modes indicated that environmental factors and shell size accounted for most of the among-site shell variations. This suggested no residual effect of species identity or hybridisation (or other potentially influential factors) on the thickness of individual shell layers at different sites after accounting for the effects of environmental conditions and shell size.

A PCA on shell traits indicated marked differences in shell composition among sites from different climatic regions (Fig. S7). PC1 captured most of the shell variation among induvial (74.7%) indicating differences in shell composition due to the wide range of size classes (shell length) available. PC2 (16.9%) indicating formation of shells with thicker periostracum in low-salinity environments (polar and Baltic region). PC3 (8.36%) captured heterogeneous within-region variations in prismatic and nacreous layers deposition, supporting no change in the relative deposition of calcareous shell components with latitude.

DISCUSSION

Our results demonstrate that plasticity in shell biomineralisation in *Mytilus* species shapes regional differences in shell production and composition as a response to the spatial structure of environmental conditions. An understanding of the biological processes driving differences in responses of species among regions to multiple interacting stressors is crucial for improving

predictive accuracy and informing more realistic projections of species and ecosystem resilience to climate change (Urban et al., 2016). Heterogeneous population-level responses from different climates act as a natural laboratory for investigating potential effects of future change. These differing responses suggest salinity is the best predictor of within-region variations in *Mytilus* shell production, mineral (prismatic and nacreous layers) and organic (periostracum) composition during growth. Spatial variations and trade-offs in shell biomineralisation suggest geographic differences in chemical and mechanical protection, shaping spatial patterns of resistance of these foundation species to global environmental changes.

Decreasing shell calcification (increasing organic content and thinner shells) towards high latitudes (Fig. 2, 3) supports documented patterns of skeletal production and estimated costs (Watson et al., 2017, 2012). Two explanatory paradigms exist for decreased skeletal size at higher latitudes: i) increased calcification costs due to poleward decrease in Ω_{CaCO_3} and reduced ectotherms metabolic rate (Watson et al., 2017, 2012) and ii) reduced predation pressure of durophagous (shell crushing) and drilling predators (e.g. crabs, dog whelks and seabirds) (Aronson et al., 2007; Harper & Peck, 2016). Given the higher production cost of shell organics than $CaCO_3$ deposition (Palmer, 1992; Sanders et al., 2018; Watson et al., 2017) and problematic protein production at polar temperatures (Peck, 2016, 2018), we might expect a reduced proportion of organic matrix. Moreover, decreasing predation pressure should result in thinner shells (Freeman, 2007; Sherker, Ellrich, & Scrosati, 2017) of the same composition irrespective of geographic area. However, the wt% of organic matrix was higher at Arctic latitudes. This could suggest either a marked increase in the cost of calcification in polar regions (Watson et al., 2017), altering significantly the relative costs of organics and $CaCO_3$ production (Sanders et al., 2018), or seawater Ω_{CaCO_3} below one ($\Omega \leq 1$) due to low temperatures and salinity

thermodynamically favouring net dissolution of $CaCO_3$ structures (Ries et al., 2016; Thomsen et al., 2018). In either case, these effects would result in decreased shell calcification at high latitudes. Increased proportions of insoluble organic matrix, which protects the calcified shell components from dissolution (Harper, 2000), and deposition of thinner shells suggest a trade-off between potential resilience to dissolving conditions and increased vulnerability to predators. This may have adaptive beneficial effects on mussels in more corrosive, polar and subpolar waters where predation pressure is low.

For over 60 years, temperature and shell size have been considered primary drivers of biogenic $CaCO_3$ mineralogy across latitudes, dictating the formation of predominantly aragonitic structures in temperate regions and increased calcite precipitation in cold climates (Carter & Seed, 1998; Lowenstam, 1954; Ramajo, Rodriguez-Navarro, Duarte, Lardies, & Lagos, 2015). Although our study partly corroborates previous findings, we observed no significant change in the relative deposition of calcite (prismatic layer) and aragonite (nacreous layer) with latitude or temperature. But we demonstrate that salinity had the strongest effect on shell production and composition in Atlantic *Mytilus* (Fig. 2), supporting the strong influence of salinity on water carbonate chemistry (Ω_{CaCO_3}) and calcification costs (Sanders et al., 2018; Thomsen, et al., 2015; Thomsen et al., 2018).

The interaction between shell layer, salinity and shell size (Equation 2) indicates changes in shell production (quantity) and composition (quality) in *Mytilus* spp. across different salinities (Fig. 4). Shifts in shell structure from juveniles to large adults lead to the formation of thinner, prismatic-dominated shells in brackish waters and thicker, nacre-dominated structures under marine conditions (Fig. 4b,c). Observed variations in predominant shell mineralogy with salinity regime, suggest changes most likely driven by altered seawater carbonate saturation state. Low

474 temperatures and salinities in polar and subpolar regions, relative to temperate areas, would lead
475 to lower Ω_{CaCO_3} and favour net dissolution of the less stable of the two main forms of $CaCO_3$,
476 the aragonite (Mucci, 1983; Ries et al., 2016; Thomsen, et al., 2015), with formation of thinner,
477 calcite-dominated shells. Conversely, in temperate Atlantic regions, warmer and saltier waters
478 (higher Ω_{CaCO_3}) are less likely to constrain $CaCO_3$ production and deposition of thicker shells.
479 Very low salinities in the Baltic Sea, compared to the mean oceanic salinity, correlate with
480 limiting concentrations of calcification substrates (Thomsen et al., 2018) and lead to extended
481 period of aragonite undersaturation ($\Omega_{arag} < 1$), imposing kinetic constraints on calcification
482 (Tyrrell, Schneider, Charalampopoulou, & Riebesell, 2008). This will likely increase energetic
483 costs of calcification (Sanders et al., 2018; Thomsen et al., 2018) and favour net dissolution of
484 aragonite over calcite structures with formation of thinner shells characterised by higher
485 proportions of calcite (Melzner et al., 2011). No difference in site-level effects on individual
486 layers was found, suggesting modelled shell variations are independent of species identity and
487 hybridisation (Fig. 5b). This supports the relatively smaller contribution of genetic status than
488 environmental heterogeneity on the variability of *Mytilus* shell traits across large-geographic
489 scales suggested by Krapivka et al. (2007) and Telesca et al. (2018). Observed response patterns
490 suggest a strong potential for qualitative and quantitative shell adjustments in blue mussels to
491 produce the most appropriate shell structure for specific environmental conditions.

492 Under current scenarios, plasticity in shell biomineralisation could represent an advantageous
493 compensatory mechanism for *Mytilus* species when facing different water chemistries and
494 predation levels. In fact, at high-latitudes and in the Baltic region, where durophagous predators
495 are rare or absent (Aronson et al., 2007; Harper & Peck, 2016; Kautsky, Johannesson, &
496 Tedengren, 1990; Reimer & Harms-Ringdahl, 2001) and the water is more likely to constrain

497 $CaCO_3$ deposition ($\Omega_{CaCO_3} \leq 1$) (Watson et al., 2017), mussels are characterised by thinner,
498 prismatic-dominated (calcitic) shells enriched in organic matrix, providing a generally higher
499 protection from dissolution (Harper, 2000; Mucci, 1983). Conversely, at mid-latitudes, where
500 durophagous predators are more abundant (Harper & Peck, 2016; MacArthur, 1972) and
501 Ω_{CaCO_3} is generally higher (Watson et al., 2017), mussels display thicker, nacre-dominated
502 (aragonitic) shells suggesting higher mechanical resistance to predation (Barthelat et al., 2009;
503 Lowen, Innes, & Thompson, 2013; Sherker et al., 2017).

504 Despite projected global changes in salinity gradients (Durack et al., 2012), *Mytilus* species show
505 a strong capacity for compensatory responses in shell production to mitigate the emergent
506 negative effects of changing water chemistry. In fact, the interacting effects of salinity, shell
507 length, and a minor influence of temperature on the periostracum (Fig. 5a, S6), which represents
508 a strong chemical barrier to shell dissolution in molluscs (Harper, 1997; Peck, Tarling, Manno,
509 Harper, & Tynan, 2016; Tunnicliffe et al., 2009), indicated deposition of thicker periostraca
510 under decreasing salinities. This likely increases the durability of periostracum to environmental
511 abrasion during aging and better mediates impacts of ocean acidification.

512 Although populations in high-latitude ecosystems will experience globally the most rapid
513 acidification (Gattuso et al., 2015), decreasing salinity (lower Ω_{CaCO_3}) predicts deposition of
514 thinner shells with an increased proportion of organic-enriched, prismatic layers and thicker
515 periostraca, potentially increasing shell resistance to future more corrosive conditions.
516 Conversely, in temperate areas, increasing salinity (higher Ω_{CaCO_3}) predicts deposition of thicker
517 shells with relatively thicker nacreous layers, favouring mechanical protection from higher
518 predation pressure in warmer climates (Freeman, 2007; Harper & Peck, 2016; Lowen et al.,

519 2013; Sherker et al., 2017). However, forecasted changes in the thickness of periostracum with
520 salinity depend on shell size and would be more evident in larger or faster growing individuals
521 (length > 48 mm) (Fig. 5a).

522 In Greenland, where the rate of melting of the ice sheet has doubled in the last decade (Kjeldsen
523 et al., 2015), lower salinities during summer (< 20 psu) (Sejr et al., 2017), decreasing Ω_{CaCO_3} and
524 increasing primary productivity (food supply) in coastal areas (Meire et al., 2017), predict
525 formation of thicker periostraca and proportionally thicker organic-enriched calcitic layers.
526 These shell adjustments in Arctic *Mytilus* spp. could represent compensatory responses for a
527 potentially increased resilience to future water conditions favouring shell dissolution at the price
528 of decreased protection from predators. In contrast, in the Baltic Sea, the projected decrease in
529 salinity (up to 45% reduction in the north-eastern and central Baltic) (Gräwe, Friedland, &
530 Burchard, 2013), combined with the considerable physiological osmotic stress (salinity from 22
531 psu to 3 psu), would be particularly critical for mussels inhabiting already unfavourable
532 conditions for calcification (i.e. limiting $[Ca^{2+}]$ and aragonite undersaturated seawater) (Sanders
533 et al., 2018; Thomsen et al., 2018). Moreover, the reduced shell size of Baltic *Mytilus* does not
534 predict formation of thicker, durable periostraca, which could further increase vulnerability to
535 dissolution. Impacts of changing salinity on *Mytilus*, which contributes up to 90% of the Baltic
536 benthic invertebrate biomass (Kautsky et al., 1990), could have large-scale implications for
537 coastal communities in the near future (Johannesson, Smolarz, Grahn, & André, 2011).

538 *Mytilus* species have a marked shell plasticity and thick periostracum compared to other
539 calcifiers that often compete with it for space (e.g. barnacles and spirorbid polychaetes).
540 Biomineralisation plasticity may act as a mechanism conferring *Mytilus* species a protective
541 capacity for quantitative and qualitative trade-offs in shell deposition to produce the most

appropriate shell structure for a specific set of abiotic (i.e. $CaCO_3$ water chemistry and sources) and biotic (i.e. predation pressure) conditions. This potential mechanism could represent a major factor for keystone calcifiers, not only molluscs, to maintain their ecological role and functions in rapidly changing oceans. Moreover, the periostracum provides a strong defence against shell dissolution and allows mytilids to survive in oligohaline waters (~5 psu) and extremely acidified conditions (e.g. hydrothermal vents) (Harper, 1997; Tunnicliffe et al., 2009). These factors may shift the ecological balance and community structure in favour of species with a greater response potential and stronger resistance to corrosive conditions, such as mussels, when ocean waters become fresher and more acidic in future decades.

As hypothesised, plasticity in shell biomineralisation shapes regional differences in *Mytilus* shell responses to interacting environmental conditions and drives spatial variations of chemical and mechanical shell protection, dictating geographic patterns of Atlantic *Mytilus* sensitivity to future environmental change. Overall, mussel shell calcification decreased towards high latitudes, with salinity being the best predictor of within-region variations in shell production, mineral and organic composition. Quantitative and qualitative differences in shell deposition among regions indicate compensatory trade-offs in shell components suggesting the potential for a higher resistance against dissolution for mussels in polar, low-salinity environments, and an enhanced mechanical protection from predators in temperate, higher-salinity regions. The strong response potential of blue mussel shell periostracum suggests a potentially increased resilience to ocean acidification in polar and sub-polar *Mytilus*, and a higher sensitivity of Baltic populations under future environmental conditions.

Our findings indicates that a better understanding of key biological processes mediating species' response to habitat alterations will be essential for identifying vulnerability and informing

conservation practices, especially for species having both high climate sensitivity and key ecological roles in shaping marine communities. This knowledge underpins our ability to predict accurately and reduce the damaging effect of climate change on future biodiversity under any range of scenarios (Urban et al., 2016). Our study has important implications because it explores the links between i) the mechanisms of biological variation, as biomineralisation plasticity, ii) species' responses to the spatial co-occurrence of multiple environmental drivers, and iii) potential regional differences in resilience of calcifying species to habitat change. This understanding is of critical importance for making realistic projections of emergent ecological effects of global environmental changes, such as altered salinity regimes, and to improve our predictive accuracy for impacts on marine communities and ecosystems, and the services they provide.

ACKNOWLEDGMENTS

We thank Iain Johnston (Scottish Oceans Institute, St. Andrews, UK), Sarah Dashfield (Plymouth Marine Laboratory, Plymouth, UK), Dr Peter Thor (Norwegian Polar Institute, Tromsø, Norway), Dr Alexander Ventura (University of Gothenburg, Kristineberg, Sweden), Prof Joseph Hoffman (Bielefeld University, Bielefeld, Germany), Dr Henk van der Veer and Rob Dekker (Royal Netherlands Institute for Sea Research, Texel, Netherlands) for help with specimens collection. We also thank Prof. Michael Carpenter (University of Cambridge, UK) for help with furnace analyses and the Statistics Clinic (University of Cambridge, UK) for statistical advice. The work was funded by the European Union Seventh Framework Programme, Marie Curie ITN CAlcium in a CHanging Environment (CACHE), under grant agreement n° 605051.

JT acknowledges additional financial support from the Independent Research Fund Denmark, DFF-International Post-doc Grant n° 7027-00060B.

REFERENCES

Aronson, R. B., Thatje, S., Clarke, A., Peck, L. S., Blake, D. B., Wilga, C. D., & Seibel, B. A. (2007). Climate change and invasibility of the Antarctic benthos. *Annual Review of Ecology, Evolution, and Systematics*, *38*(1), 129–154.

Ashton, G. V., Morley, S. A., Barnes, D. K. A., Clark, M. S., & Peck, L. S. (2017). Warming by 1 °C drives species and assemblage level responses in Antarctica's marine shallows. *Current Biology*, *27*(17), 2698-2705.e3.

Barthelat, F., Rim, J. E., & Espinosa, H. D. (2009). A review on the structure and mechanical properties of mollusk shells – Perspectives on synthetic biomimetic materials. In B. Bhushan & H. Fuchs (Eds.), *Applied Scanning Probe Methods XIII* (pp. 17–44). Berlin, Heidelberg: Springer.

Bolker, B. M. (2015). Linear and generalized linear mixed models. In G. A. Fox, S. Negrete-Yankelevich, & V. J. Sosa (Eds.), *Ecological Statistics* (pp. 309–333). Oxford, UK: Oxford University Press.

Breitburg, D. L., Salisbury, J., Bernhard, J., Cai, W.-J., Dupont, S., Doney, S., … Tarrant, A. (2015). And on top of all that… Coping with ocean acidification in the midst of many stressors. *Oceanography*, *28*(2), 48–61.

Burnham, K. P., & Anderson, D. R. (2002). *Model Selection and Multimodel Inference : a Practical Information-Theoretic Approach*. New York, NY, USA: Springer-Verlag.

Calosi, P., Melatunan, S., Turner, L. M., Artioli, Y., Davidson, R. L., Byrne, J. J., … Rundle, S. D. (2017). Regional adaptation defines sensitivity to future ocean acidification. *Nature Communications*, *8*, 13994.

Carter, J. G., & Seed, R. (1998). Thermal potentiation and mineralogical evolution in *Mytilus* (Mollusca; Bivalvia). In P. A. Johnston & J. W. Haggart (Eds.), *Bivalves: an Eon of Evolution* (pp. 87–117). Vancouver: University of Calgary Press.

Checa, A. G., Macías-Sánchez, E., Harper, E. M., & Cartwright, J. H. E. (2016). Organic membranes determine the pattern of the columnar prismatic layer of mollusc shells. *Proceedings of the Royal Society B*, *283*(1830), 20160032.

Checa, A. G., Pina, C. M., Osuna-Mascaró, A. J., Rodríguez-Navarro, A. B., & Harper, E. M. (2014). Crystalline organization of the fibrous prismatic calcitic layer of the Mediterranean mussel *Mytilus galloprovincialis*. *European Journal of Mineralogy*, *26*(4), 495–505.

Connell, S. D., Doubleday, Z. A., Hamlyn, S. B., Foster, N. R., Harley, C. D. G., Helmuth, B., … Russell, B. D. (2017). How ocean acidification can benefit calcifiers. *Current Biology*, *27*(3), R95–R96.

Crain, C. M., Kroeker, K., & Halpern, B. S. (2008). Interactive and cumulative effects of multiple human stressors in marine systems. *Ecology Letters*, *11*(12), 1304–1315.

Cross, E. L., Harper, E. M., & Peck, L. S. (2019). Thicker shells compensate extensive

dissolution in brachiopods under future ocean scidification. *Environmental Science & Technology*, *53*(9), 5016–5026.

Currey, J. D., & Taylor, J. D. (1974). The mechanical behaviour of some molluscan hard tissues. *Journal of Zoology*, *173*(3), 395–406.

Durack, P. J., Wijffels, S. E., & Matear, R. J. (2012). Ocean salinities reveal strong global water cycle intensification during 1950 to 2000. *Science*, *336*(6080), 455–458.

FAO. (2017). *FAO Yearbook. Fishery and Aquaculture Statistics. 2015*. Rome: FAO.

Fitzer, S. C., Zhu, W., Tanner, K. E., Phoenix, V. R., Kamenos, N. A., & Cusack, M. (2015). Ocean acidification alters the material properties of *Mytilus edulis* shells. *Journal of the Royal Society, Interface*, *12*(103), 20141227.

Freeman, A. S. (2007). Specificity of induced defenses in *Mytilus edulis* and asymmetrical predator deterrence. *Marine Ecology Progress Series*, *334*, 145–153.

Gattuso, J. P., Magnan, A., Bille, R., Cheung, W. W. L., Howes, E. L., Joos, F., … Turley, C. (2015). Contrasting futures for ocean and society from different anthropogenic CO_2 emissions scenarios. *Science*, *349*(6243), aac4722.

Ghedini, G., Russell, B. D., & Connell, S. D. (2015). Trophic compensation reinforces resistance: herbivory absorbs the increasing effects of multiple disturbances. *Ecology Letters*, *18*(2), 182–187.

Graham, M. H. (2003). Confronting multicollinearity in ecological multiple regression. *Ecology*, *84*(11), 2809–2815.

Gräwe, U., Friedland, R., & Burchard, H. (2013). The future of the western Baltic Sea: two possible scenarios. *Ocean Dynamics*, *63*(8), 901–921.

Grueber, C. E., Nakagawa, S., Laws, R. J., & Jamieson, I. G. (2011). Multimodel inference in ecology and evolution: challenges and solutions. *Journal of Evolutionary Biology*, *24*(4), 699–711.

Harper, E. M. (1997). The molluscan periostracum: an important constraint in bivalve evolution. *Palaeontology*, *40*(1), 71–97.

Harper, E. M. (2000). Are calcitic layers an effective adaptation against shell dissolution in the Bivalvia? *Journal of Zoology*, *251*(2), 179–186.

Harper, E. M., & Peck, L. S. (2016). Latitudinal and depth gradients in marine predation pressure. *Global Ecology and Biogeography*, *25*(6), 670–678.

IOCCG. (2014). *Phytoplankton Functional Types from Space. Reports of the International Ocean-Colour Coordinating Group, No. 15*. (S. Sathyendranath, Ed.). Dartmouth: IOCCG.

Johannesson, K., Smolarz, K., Grahn, M., & André, C. (2011). The future of Baltic Sea populations: Local extinction or evolutionary rescue? *AMBIO*, *40*(2), 179–190.

Kautsky, N., Johannesson, K., & Tedengren, M. (1990). Genotypic and phenotypic differences between Baltic and North Sea populations of *Mytilus edulis* evaluated through reciprocal transplantations. I Growth and morphology. *Marine Ecology Progress Series*, *59*, 203–210.

Kirtman, B., Power, S. B., Adedoyin, J. A., Boer, G. J., Bojariu, R., Camilloni, I., … Wang, H. J. (2013). Near-term climate change: projections and predictability. In T. F. Stocker, D. Qin,

G.-K. Plattner, M. Tignor, S. K. Allen, J. Boschung, … P. M. Midgley (Eds.), *Climate Change 2013: The Physical Science Basis. Contribution of Working Group I to the Fifth Assessment Report of the Intergovernmental Panel on Climate Change* (pp. 953–1028). Cambridge, UK: Cambridge University Press.

Kjeldsen, K. K., Korsgaard, N. J., Bjørk, A. A., Khan, S. A., Box, J. E., Funder, S., … Kjær, K. H. (2015). Spatial and temporal distribution of mass loss from the Greenland Ice Sheet since AD 1900. *Nature*, *528*(7582), 396–400.

Krapivka, S., Toro, J. E., Alcapán, A. C., Astorga, M., Presa, P., Pérez, M., & Guiñez, R. (2007). Shell-shape variation along the latitudinal range of the Chilean blue mussel *Mytilus chilensis* (Hupé 1854). *Aquaculture Research*, *38*(16), 1770–1777.

Kroeker, K. J., Kordas, R. L., Crim, R., Hendriks, I. E., Ramajo, L., Singh, G. S., … Gattuso, J.-P. (2013). Impacts of ocean acidification on marine organisms: quantifying sensitivities and interaction with warming. *Global Change Biology*, *19*(6), 1884–1896.

Kroeker, K. J., Kordas, R. L., & Harley, C. D. G. (2017). Embracing interactions in ocean acidification research: Confronting multiple stressor scenarios and context dependence. *Biology Letters*, *13*(3), 20160802.

Kroeker, K. J., Sanford, E., Rose, J. M., Blanchette, C. A., Chan, F., Chavez, F. P., … Washburn, L. (2016). Interacting environmental mosaics drive geographic variation in mussel performance and predation vulnerability. *Ecology Letters*, *19*(7), 771–779.

Leung, J. Y. S., Russell, B. D., & Connell, S. D. (2017). Mineralogical plasticity acts as a compensatory mechanism to the impacts of ocean acidification. *Environmental Science &*

Technology, *51*(5), 2652–2659.

Lowen, J., Innes, D., & Thompson, R. (2013). Predator-induced defenses differ between sympatric *Mytilus edulis* and *M. trossulus*. *Marine Ecology Progress Series*, *475*, 135–143.

Lowenstam, H. A. (1954). Factors affecting the aragonite:calcite ratios in carbonate-secreting marine organisms. *The Journal of Geology*, *62*(3), 284–322.

MacArthur, R. H. (1972). *Geographical Ecology : Patterns in the Distribution of Species*. Princeton, NJ, USA: Princeton University Press.

Meire, L., Mortensen, J., Meire, P., Juul-Pedersen, T., Sejr, M. K., Rysgaard, S., … Meysman, F. J. R. (2017). Marine-terminating glaciers sustain high productivity in Greenland fjords. *Global Change Biology*, *23*(12), 5344–5357.

Melzner, F., Stange, P., Trübenbach, K., Thomsen, J., Casties, I., Panknin, U., … Gutowska, M. a. (2011). Food supply and seawater pCO_2 impact calcification and internal shell dissolution in the blue mussel *Mytilus edulis*. *PLoS ONE*, *6*(9), e24223.

Mucci, A. (1983). The solubility of calcite and aragonite in seawater at various salinities, temperatures, and one atmosphere total pressure. *American Journal of Science*, *283*(7), 780–799.

Nagelkerken, I., & Connell, S. D. (2015). Global alteration of ocean ecosystem functioning due to increasing human CO_2 emissions. *Proceedings of the National Academy of Sciences of the United States of America*, *112*(43), 13272–13277.

Nakagawa, S., Johnson, P. C. D., & Schielzeth, H. (2017). The coefficient of determination R^2

and intra-class correlation coefficient from generalized linear mixed-effects models revisited and expanded. *Journal of The Royal Society Interface*, *14*(134), 20170213.

Palmer, A. R. (1992). Calcification in marine molluscs: how costly is it? *Proceedings of the National Academy of Sciences of the United States of America*, *89*(4), 1379–1382.

Peck, L. S. (2016). A cold limit to adaptation in the sea. *Trends in Ecology & Evolution*, *31*(1), 13–26.

Peck, L. S. (2018). Antarctic marine biodiversity: adaptations, environments and responses to change. In S. J. Hawkins, A. J. Evans, A. C. Dal, L. B. Firth, & I. P. Smith (Eds.), *Oceanography and Marine Biology: an Annual Review* (Vol. 56, p. 510). CRC Press.

Peck, L. S., Clark, M. S., Power, D., Reis, J., Batista, F. M., & Harper, E. M. (2015). Acidification effects on biofouling communities: winners and losers. *Global Change Biology*, *21*(5), 1907–1913.

Peck, V. L., Tarling, G. A., Manno, C., Harper, E. M., & Tynan, E. (2016). Outer organic layer and internal repair mechanism protects pteropod *Limacina helicina* from ocean acidification. *Deep Sea Research Part II: Topical Studies in Oceanography*, *127*, 41–52.

Ramajo, L., Rodriguez-Navarro, A. B., Duarte, C. M., Lardies, M. A., & Lagos, N. A. (2015). Shifts in shell mineralogy and metabolism of *Concholepas concholepas* juveniles along the Chilean coast. *Marine and Freshwater Research*, *66*(12), 1147–1157.

Reimer, O., & Harms-Ringdahl, S. (2001). Predator-inducible changes in blue mussels from the predator-free Baltic Sea. *Marine Biology*, *139*(5), 959–965.

728 Ries, J. B., Ghazaleh, M. N., Connolly, B., Westfield, I., & Castillo, K. D. (2016). Impacts of
729 seawater saturation state (Ω_A= 0.4–4.6) and temperature (10, 25 °C) on the dissolution
730 kinetics of whole-shell biogenic carbonates. *Geochimica et Cosmochimica Acta*, *192*, 318–
731 337.

732 Riginos, C., & Cunningham, C. W. (2005). Local adaptation and species segregation in two
733 mussel (*Mytilus edulis* × *Mytilus trossulus*) hybrid zones. *Molecular Ecology*, *14*(2), 381–
734 400.

735 Sanders, T., Schmittmann, L., Nascimento-Schulze, J. C., & Melzner, F. (2018). High
736 calcification costs limit mussel growth at low salinity. *Frontiers in Marine Science*, *5*, 352.

737 Schielzeth, H. (2010). Simple means to improve the interpretability of regression coefficients.
738 *Methods in Ecology and Evolution*, *1*(2), 103–113.

739 Seed, R., & Richardson, C. A. (1990). *Mytilus* growth and its environmental responsiveness. In
740 G. B. Stefano (Ed.), *The Neurobiology of Mytilus edulis* (pp. 1–37). Manchester, UK:
741 Manchester University Press.

742 Sejr, M. K., Stedmon, C. A., Bendtsen, J., Abermann, J., Juul-Pedersen, T., Mortensen, J., &
743 Rysgaard, S. (2017). Evidence of local and regional freshening of Northeast Greenland
744 coastal waters. *Scientific Reports*, *7*(1), 13183.

745 Sherker, Z., Ellrich, J., & Scrosati, R. (2017). Predator-induced shell plasticity in mussels hinders
746 predation by drilling snails. *Marine Ecology Progress Series*, *573*, 167–175.

747 Solan, M., & Whiteley, N. (2016). *Stressors in the Marine Environment*. Oxford, UK: Oxford

University Press.

Stuckas, H., Stoof, K., Quesada, H., & Tiedemann, R. (2009). Evolutionary implications of discordant clines across the Baltic *Mytilus* hybrid zone (*Mytilus edulis* and *Mytilus trossulus*). *Heredity*, *103*(2), 146–156.

Telesca, L., Michalek, K., Sanders, T., Peck, L. S., Thyrring, J., & Harper, E. M. (2018). Blue mussel shell shape plasticity and natural environments: a quantitative approach. *Scientific Reports*, *8*(1), 2865.

Thomas, Y., Mazurié, J., Alunno-Bruscia, M., Bacher, C., Bouget, J.-F., Gohin, F., … Struski, C. (2011). Modelling spatio-temporal variability of *Mytilus edulis* (L.) growth by forcing a dynamic energy budget model with satellite-derived environmental data. *Journal of Sea Research*, *66*(4), 308–317.

Thomsen, J., Casties, I., Pansch, C., Körtzinger, A., & Melzner, F. (2013). Food availability outweighs ocean acidification effects in juvenile *Mytilus edulis*: laboratory and field experiments. *Global Change Biology*, *19*(4), 1017–1027.

Thomsen, J., Gutowska, M. A., Saphorster, J., Heinemann, A., Trubenbach, K., Fietzke, J., … Melzner, F. (2010). Calcifying invertebrates succeed in a naturally CO_2-rich coastal habitat but are threatened by high levels of future acidification. *Biogeosciences*, *7*(11), 3879–3891.

Thomsen, J., Haynert, K., Wegner, K. M., & Melzner, F. (2015). Impact of seawater carbonate chemistry on the calcification of marine bivalves. *Biogeosciences*, *12*(14), 4209–4220.

Thomsen, J., Ramesh, K., Sanders, T., Bleich, M., & Melzner, F. (2018). Calcification in a

marginal sea – influence of seawater [Ca^{2+}] and carbonate chemistry on bivalve shell formation. *Biogeosciences*, *15*(5), 1469–1482.

Thomsen, J., Stapp, L. S., Haynert, K., Schade, H., Danelli, M., Lannig, G., … Melzner, F. (2017). Naturally acidified habitat selects for ocean acidification – tolerant mussels. *Science Advances*, *3*(4), e1602411.

Thyrring, J., Blicher, M., Sørensen, J., Wegeberg, S., & Sejr, M. (2017). Rising air temperatures will increase intertidal mussel abundance in the Arctic. *Marine Ecology Progress Series*, *584*, 91–104.

Tunnicliffe, V., Davies, K. T. A., Butterfield, D. A., Embley, R. W., Rose, J. M., & Chadwick Jr, W. W. (2009). Survival of mussels in extremely acidic waters on a submarine volcano. *Nature Geoscience*, *2*(5), 344–348.

Tyrrell, T., Schneider, B., Charalampopoulou, A., & Riebesell, U. (2008). Coccolithophores and calcite saturation state in the Baltic and Black Seas. *Biogeosciences*, *5*(2), 485–494.

Urban, M. C., Bocedi, G., Hendry, A. P., Mihoub, J.-B., Peer, G., Singer, A., … Travis, J. M. J. (2016). Improving the forecast for biodiversity under climate change. *Science*, *353*(6304), aad8466.

Vargas, C. A., Lagos, N. A., Lardies, M. A., Duarte, C., Manríquez, P. H., Aguilera, V. M., … Dupont, S. (2017). Species-specific responses to ocean acidification should account for local adaptation and adaptive plasticity. *Nature Ecology & Evolution*, *1*(4), 0084.

Watson, S.-A., Morley, S. A., & Peck, L. S. (2017). Latitudinal trends in shell production cost

from the tropics to the poles. *Science Advances*, *3*(9), e1701362.

Watson, S.-A., Peck, L. S., Tyler, P. A., Southgate, P. C., Tan, K. S., Day, R. W., & Morley, S. A. (2012). Marine invertebrate skeleton size varies with latitude, temperature and carbonate saturation: implications for global change and ocean acidification. *Global Change Biology*, *18*(10), 3026–3038.

Zaremba, C. M., Morse, D. E., Mann, S., Hansma, P. K., & Stucky, G. D. (1998). Aragonite−hydroxyapatite conversion in gastropod (Abalone) nacre. *Chemistry of Materials*, *10*(12), 3813–3824.

Zuur, A. F., Ieno, E. N., & Elphick, C. S. (2010). A protocol for data exploration to avoid common statistical problems. *Methods in Ecology and Evolution*, *1*(1), 3–14.

Zuur, A. F., Ieno, E. N., Walker, N., Saveliev, A. A., & Smith, G. M. (2009). *Mixed Effects Models and Extensions in Ecology with R*. New York, NY: Springer New York.

TABLES

Table 1. Environmental GLMMs summary.

Estimated statistics and bootstrapped 95% CIs for regression parameters are reported for the modelled relationships between thickness of the various shell layers and whole-shell against standardised covariates. For the summary of model in Equation (1), estimates for group means, slopes, and standard errors are reported separately for the prismatic and nacreous layers (Table S6). (Parameters' significance is determined when the 95% CI does not include zero).

	Estimate	SE	95% CI	*t*-value	*p*-value (approximate)
Whole-shell*					
(Intercept)	6.617	0.051	**6.517**; **6.717**	128.71	<**0.0001**
Temperature	0.156	0.054	**0.014**; **0.240**	2.89	**0.013**
Salinity	0.525	0.060	**0.411**; **0.672**	8.69	<**0.0001**
Chl-*a*	0.074	0.054	-0.042; 0.216	1.37	0.20
Length	0.248	0.037	**0.181**; **0.327**	6.44	<**0.0001**
Prismatic (Pr) & nacreous (Na)†					
(Intercept)Layer(Pr)	5.907	0.031	**5.775**; **6.038**	188.31	<**0.0001**
(Intercept)Layer(Na)	5.853	0.083	**5.715**; **5.990**	70.81	<**0.0001**
Temperature	0.138	0.033	**0.016**; **0.263**	4.17	**0.0008**
Chl-*a*	0.028	0.033	-0.084; 0.141	0.86	0.40
Salinity × Layer(Pr)	0.396	0.039	**0.262**; **0.529**	10.22	<**0.0001**
Salinity × Layer(Na)	0.654	0.093	**0.501**; **0.811**	7.07	<**0.0001**
Length × Layer(Pr)	0.197	0.031	**0.094**; **0.295**	6.39	<**0.0001**
Length × Layer(Na)	0.308	0.065	**0.196**; **0.419**	4.74	<**0.0001**
Periostracum‡					
(Intercept)	3.500	0.048	**3.406**; **3.596**	71.03	<**0.0001**
Temperature	0.049	0.043	-0.036; 0.134	1.12	0.28
Salinity	-0.009	0.061	-0.131; 0.111	-0.14	0.89

Chl-*a*	0.147	0.038	**0.071**; **0.221**	3.88	**0.0020**
Length	0.439	0.041	**0.357**; **0.522**	10.25	<**0.0001**
Temperature × Length	-0.064	0.035	-0.135; 0.006	-1.77	0.082
Salinity × Length	-0.151	0.061	**-0.271**; **-0.029**	-2.38	**0.020**

808 * Whole-shell, the random intercept was normally distributed with mean of 0 and variance
809 0.209^2.
810 † Prismatic and nacreous layers, the random intercepts were normally distributed with mean 0,
811 and variances 0.123^2 and 0.310^2, respectively.
812 ‡ Periostracum, the random intercept was normally distributed with mean 0 and variance 0.130^2.
813

FIGURE CAPTIONS

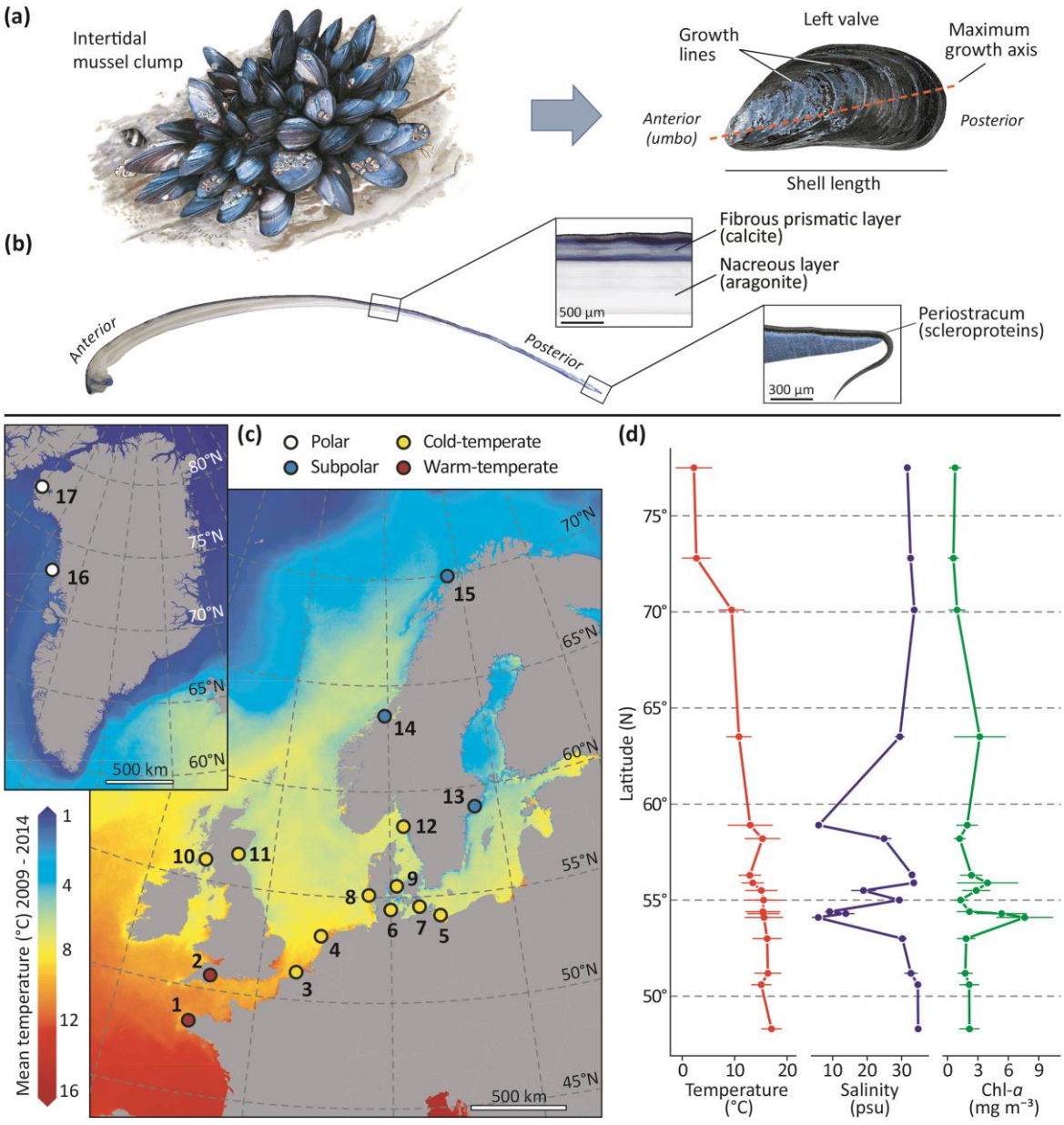

Figure 1. *Mytilus* spp. shell, collection sites and environmental heterogeneity. **(a)** *Mytilus* shell valve morphology and dimensions. **(b)** Anteroposterior cross-section of shell valve along the axis of maximum growth (from umbo to posterior commissure, dashed line) showing internal structure and composition of individual mineral (prismatic and nacreous) and organic (periostracum) shell layers. **(c)** Thermal map of North-East Atlantic and Arctic surface waters

from the CMEMS (http://marine.copernicus.eu/) biogeochemical datasets showing locations at different climatic regions (open circles) where *Mytilus* specimens were collected from across the Eastern European and Greenlandic coastlines (from 48°N to 78°N): (1) Brest, France, (2) Exmouth, England, (3) Oostende, Belgium, (4) Texel, Netherlands, (5) Usedom, (6) Kiel, (7) Ahrenshoop, (8) Sylt, all Germany, (9) Kerteminde, Denmark, (10) Tarbet, Kintyre, Scotland, (11) St. Andrews, Scotland, (12) Kristineberg, Sweden, (13) Nynäshamn, Sweden, (14) Trondhiem, Norway, (15) Tromsø, Norway, (16) Upernavik, Greenland and (17) Qaanaaq, Greenland. Map created with ArcMap 10.5 (ArcGIS software by Esri, http://esri.com), background image courtesy of OpenStreetMap (http://www.openstreetmap.org). **(d)** Heterogeneous latitudinal gradients for sea surface temperature, salinity, and Chl-*a* concentration across the study regions. Mean values (May - October, filled circles) and SD (horizontal solid lines) for the 6-year period 2009 - 2014 were estimated from CMEMS datasets.

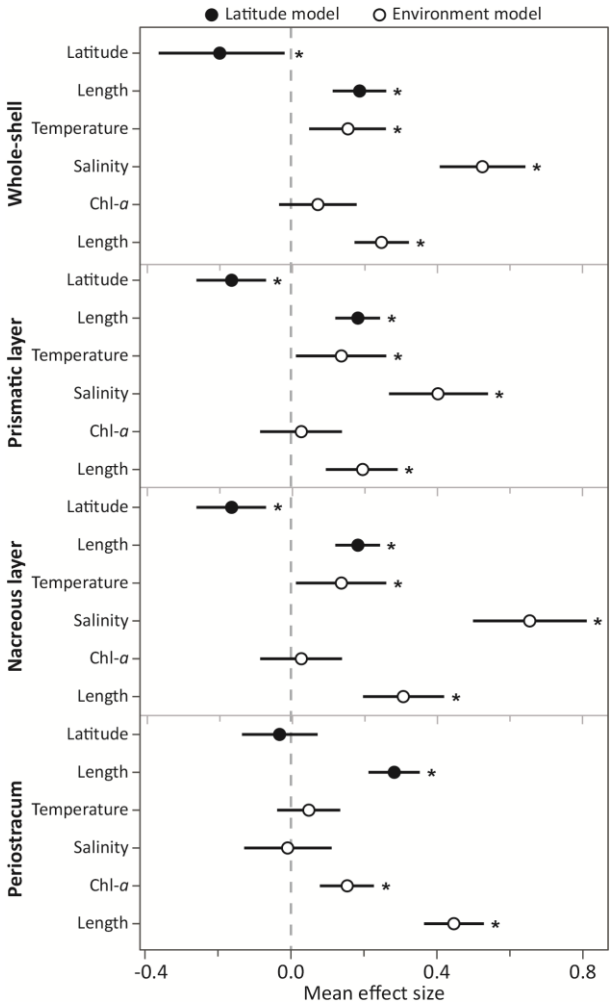

Figure 2. Mean effect size of predictors on *Mytilus* shell measurements. Effect sizes were estimated from individual latitudinal (filled circles) and environmental (open circles) GLMMs. Mean effect sizes and direction of impacts of latitude, shell length, sea surface temperature, salinity, and Chl-*a* concentration on layer ln-thickness (μm) measurements are reported for the whole-shell, prismatic layer, nacreous layer, and periostracum. Significance of regression parameters is identified when the bootstrapped 95% CI (error bars) does not cross zero (* denotes a significant difference from zero).

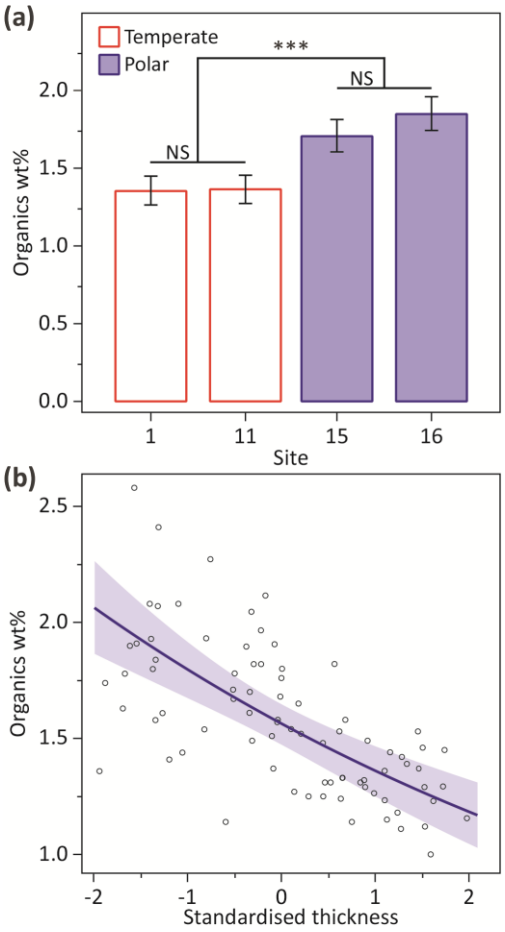

Figure 3. Latitudinal patterns of shell organic content and calcification. **(a)** Variations in organic content within prismatic layers among shells from temperate (sites 1, 11; open bars) and polar (sites 15, 16; solid bars) climates. Pair-wise contrasts indicated significantly higher proportions of organics in high-latitude than low-latitude specimens [mean difference = 0.44%; $z = 8.27$, $p < 0.0001$ (***), pseudo$R^2 = 0.49$, $n = 80$], in addition to non-significant differences (NS) among temperate (mean difference = 0.002%; $z = 0.12$, $p = 0.91$) and polar (mean difference = 0.13%, $z = 1.86$, $p = 0.063$) populations. Error bars indicate 95% CIs. **(b)** Relationship between the wt% of organics and standardised thickness of the prismatic [mean (SD) = 529 µm (174)] (sites 1, 7, 10 and 11), indicating a negative association between layer thickness and calcification level ($z =$

852 –7.10, $p < 0.0001$, pseudo$R^2 = 0.40$). Predicted values (solid line) and confidence intervals

853 (shaded area) were estimated for mussels of mean shell length (52 mm).

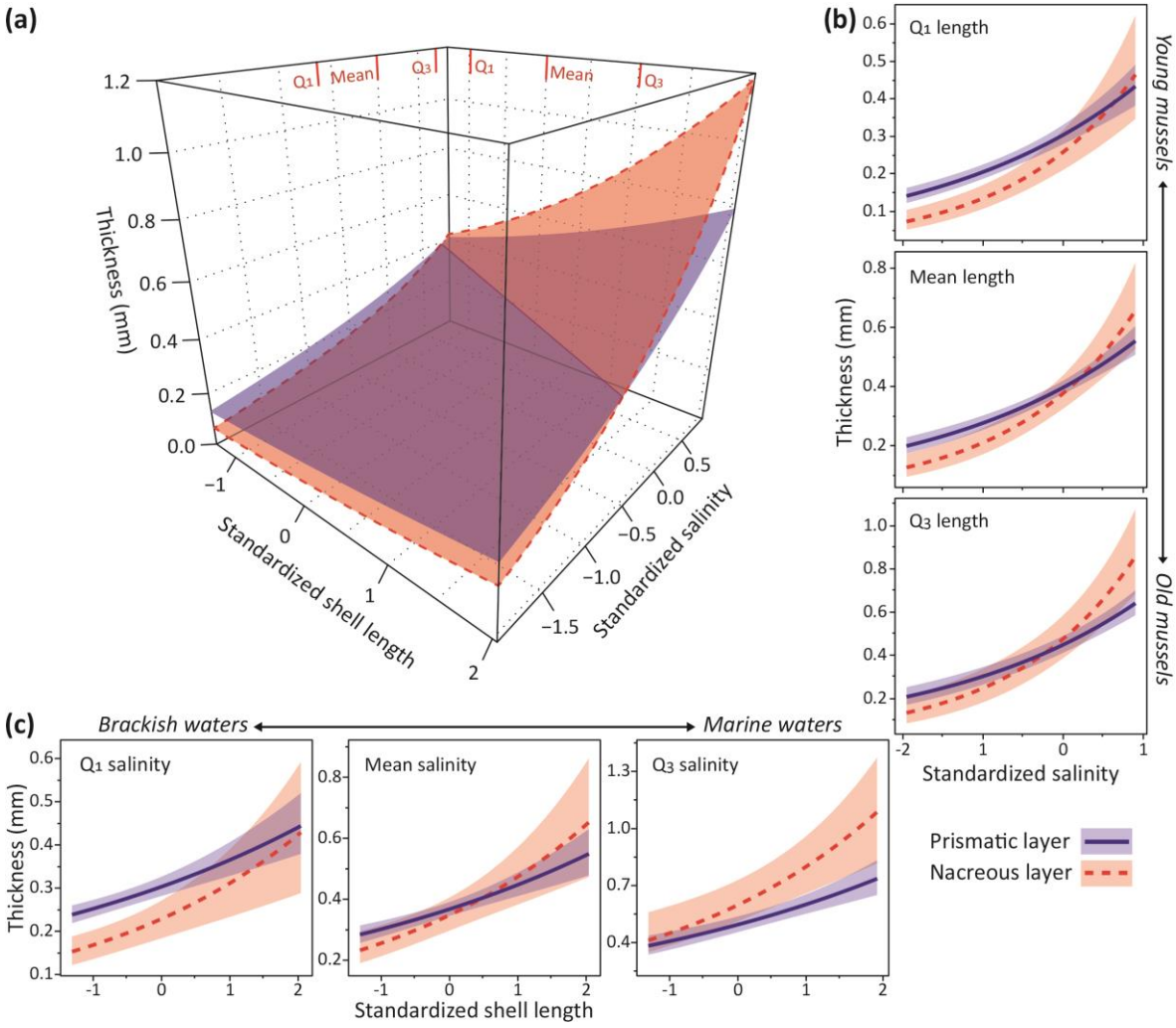

854

855 **Figure 4.** Environmental influence on shell production and composition. **(a)** Predicted multiple

856 relationships between the thickness of prismatic (solid margin plane) and nacreous (dashed

857 margin plane) layers, and standardised salinity [mean (SD) = 25.52 psu (10.29)], shell length

858 [mean (SD) = 47.42 mm (16.20)] and their interactions. **(b)** Shell thickness is modelled as a

859 function of salinity for the 1st quartile (Q_1 = 31.50 mm), mean value (47.42 mm) and 3rd quartile

860 (Q_3 = 63.90 mm) of the shell lengths sampled. For medium-sized mussels, we detected a

decreasing proportion of the prismatic layer (calcite) with increasing salinity and the deposition of relatively thicker nacreous layers (aragonite) at salinities > 27.67 psu. **(c)** Thickness is modelled as a function of length for the 1st quartile (Q_1 = 18.92 psu), mean value (25.52 psu) and 3rd quartile (Q_3 = 33.13 psu) of salinity. At mean salinity, we detected an inversion of the relative layers' thickness for shell length > 55.30 mm. Across the entire range of shell lengths, the model predicts formation of prismatic layer-dominated shells under low salinities and nacreous layer-dominated shells under higher salinities. Mean values (lines) and confidence intervals (shaded areas) are predicted while controlling for temperature (13.03 °C) and Chl-*a* (2.48 mg m^{-3}).

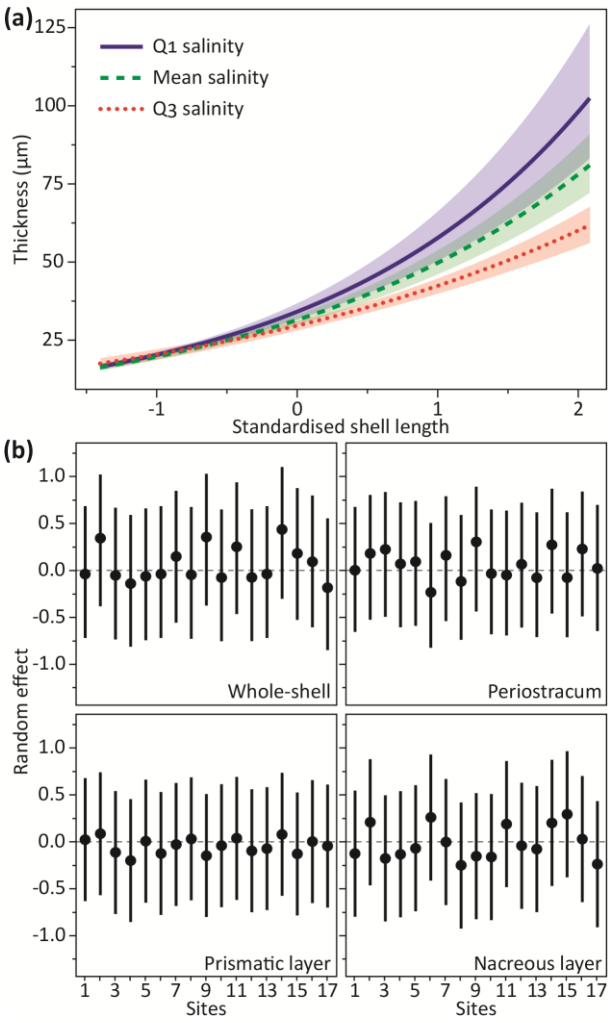

871

872 **Figure 5. (a)** Interacting effects of salinity and shell length on periostracum. Periostracum
873 thickness is modelled as a function of standardised shell length [mean (SD) = 47.42 mm (16.20)]
874 for the 1st quartile (Q_1 = 18.92 psu, solid line), mean (25.52 psu, dashed line) and 3rd quartile
875 (Q_3 = 33.13 psu, dotted line) of water salinity. Predicted values (lines) and confidence intervals
876 (shaded areas) indicate higher rates of exponential periostracal thickening with decreasing
877 salinity. Smaller individuals (shell length < 48.38 mm) were characterised by non-significant
878 thickness differences under different salinity regimes. **(b)** Among sites shell variation. GLMMs'
879 conditional modes (filled circles) and variances (solid lines) of the random effect estimated for
880 individual shell layers. Modes represent the difference between the average predicted response

881 (layer thickness) for a given set of fixed-effects values (mean environmental covariates and shell
882 length) and the response predicted at a particular site. These suggest no detectable residual effect
883 of species (*Mytilus edulis* or *M. trossulus*) and level of hybridisation on shell thickness among
884 sites.

885